

# DISCUSSION ON THE APPLICATION OF THE MEDINA MODEL TO THE FLOW CURVE OF HOT DEFORMATION

L. D. Wang<sup>1\*</sup> –X. D. Zhou<sup>1</sup>

<sup>1</sup>Material Science & Engineering College, Henan University of Science & Technology, Luo Yang 471023, People's Republic of China

---

## ARTICLE INFO

### Article history:

Received: 20.11.2012.

Received in revised form: 02.01.2013

Accepted: 15.01.2013.

### Keywords:

Median model

Flow curve

Hot forming

Fitting analysis

---

## Abstract:

*The application of the Medina model to the flow curve of hot deformation has been discussed. Using the quick fit function of 1stOpt software, the relationship between various model coefficients and a dimensionless parameter Z/A has been built. Using a classification method of the Medina model, the flow curves of 50A1300 silicon steel are built and R<sup>2</sup> of 0.979436 and the average relative error of 7,3517% are obtained. Then using a recrystallization model of the Medina model, the flow curves of 45K-DDQ are built and R<sup>2</sup> of 0,974373 and the average relative error of 6,1453% are obtained. In addition, the flow curve model is programmed in Matlab environment so that true stress could be automatically obtained. Finally, the whole fitting method and piecewise fitting method are compared when using the Medina model for solving the model parameters of the dynamic recrystallization flow curve.*

---

## 1 Introduction

The existing mathematical model referring to the flow curve of hot deformation can be divided into two categories: the one based on the macroscopic process parameters, mainly providing a basis for designing the process parameters such as in hot forging, or a mathematical model for online computer-controlled producing such as in hot rolling. Another model regards the microscopic point of view and is based on the microstructure of materials, mainly seeking the quantitative relationship between the microscopic parameters and the macroscopic stress. The mathematical models that are based on the macro mechanisms are as follows [1 - 6]: the Inoue-lang model, Ikejima-Toshio model, Teshima-Seizox model,

Misaka Kasuke model, Shida Shige model, Zhou jihua-Guan kezhi model, Cingara model, three-stage model, creep model, and Medina model [7, 8]. When the Median model was applied to a certain type of steel, how to establish the flow curve model was discussed, and the process of modeling the flow curve was analyzed in detail as well. The Medina model considers the influence of the chemical composition on the flow stress and consequently the relationship between various model parameters, chemical compositions, and also deformation parameters is gained by a regression method. The torsion test was carried out in the austenite region so that large deformation was reached and an occurrence of dynamic recrystallization was observed on the flow curves.

---

\* Corresponding author. Tel.:+86 15838526445

E-mail address: lidongwang007@gmail.com.

These flow curves are called Dynamic Recrystallization (DRX) Flow Curves which may exhibit a distinctive peak stress. By contrast, this paper, however, sets out to carry out compression tests using the Gleeble-1500D thermal simulator, the silicon steel 50A1300 (GB) and high-strength steel 45K-DDQ (GB). Gleeble-1500D, produced by DSI Corporation for physical simulation, has a high speed heating system, servo hydraulic system, computer control and data acquisition system which provide a cost effective way to physically simulate high temperature processes and applications at far lower costs than full scale tests. The obtained excellent correlation and results can then be applied to the actual process. It is worth pointing out that in the austenite region, due to the shortcomings of the compression test, some DRX flow curves in this paper did not show the peak stress even though dynamic recrystallization occurred [9]. Therefore, the Medina model was properly modified for flow curve data regression. Different methods were used and analyzed for the regression of the model parameters to solve the flow stress. Finally, the flow curve models of both steels were established.

## 1 Experimental investigation

The experimental material of 50A1300 silicon steel and 45K-DDQ high-strength steel is obtained from the actual production, and its chemical composition (wt%) is given in the Table 1. The cylindrical samples of 8 mm in diameter and 12mm in height were prepared and compression test was carried out on the Gleeble-1500D thermal simulator. The samples were deformed in an argon atmosphere. Firstly, the K-type thermal couple was welded at the half height of the cylinder. Secondly, a graphite mixture used as lubricant was applied at two ends of samples. Compression anvils were used with the purpose of minimizing the friction coefficient during hot deformation. Thirdly, the program was started after preloading. The specimens were preheated at 1200°C for 5 min and then cooled to the test temperature of 5 °C/s and held for 10 seconds prior to deformation for temperature homogenization. Tests were carried out at temperatures of 950, 1000, 1050, 1100, 1150 and 1200°C and strain rates of 0.01, 0.1, 1, 8, 15s<sup>-1</sup>. All samples were deformed up to strains of 0.9.

Table 1. Chemical ingredients of the silicon steel 50A1300 and high strength steel 45 K-DDQ

Mass fraction (%)	C	Si	Mn	P	S	Cu	Ni
45K-DDQ	0.0017	0.7	0.542	0.0865	0.0089	0.019	0.011
50A1300	0.0016	1.59	0.52	0.10	0.003		
Mass fraction (%)	Cr	Ar	Ti	Nb	V	Al	Ti
45K-DDQ	0.026	0.0026	0.002	0.0145	0.0013	0.043	0.0188
50A1300							

## 2 Results and discussion

### 2.1 The flow curves of 50A1300 silicon steel and 45K-DDQ high-strength steel

The previous papers [10, 11], offered the analyses of the effects of temperature and strain rate on the flow curve of both steels and the calculations of activation energy (Q) and the dimensionless parameter Z/A. The flow curves at strain rates of 0.01, 0.1, 1, 8 and 15 s<sup>-1</sup> were illustrated from Fig. 1 to Fig. 8.

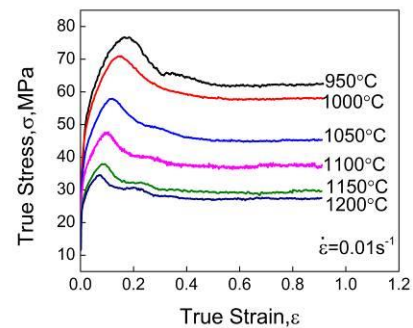


Figure 1.  $\sigma - \varepsilon$  curves at  $\dot{\varepsilon} = 0.01s^{-1}$

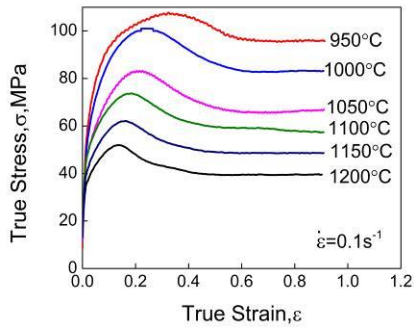


Figure 2.  $\sigma - \epsilon$  curves at  $\dot{\epsilon} = 0.1s^{-1}$

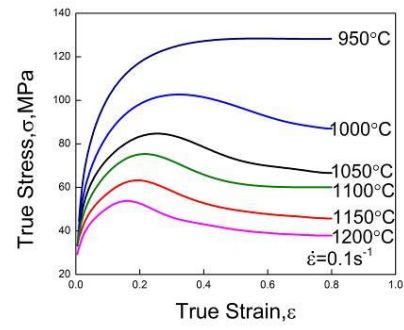


Figure 6.  $\sigma - \epsilon$  curves at  $\dot{\epsilon} = 0.1s^{-1}$

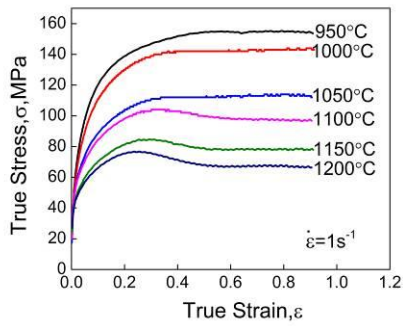


Figure 3.  $\sigma - \epsilon$  curves at  $\dot{\epsilon} = 1s^{-1}$

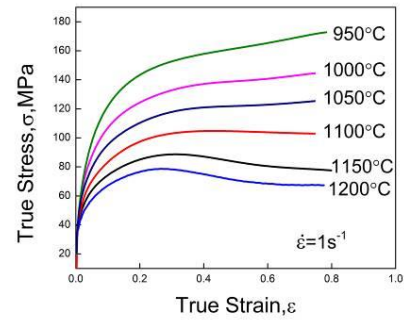


Figure 7.  $\sigma - \epsilon$  curves at  $\dot{\epsilon} = 1s^{-1}$

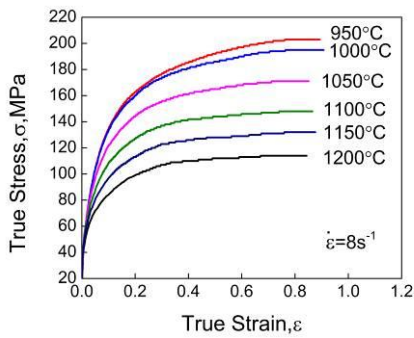


Figure 4.  $\sigma - \epsilon$  curves at  $\dot{\epsilon} = 8s^{-1}$

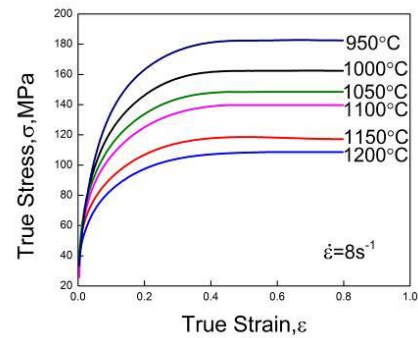


Figure 8.  $\sigma - \epsilon$  curves at  $\dot{\epsilon} = 8s^{-1}$

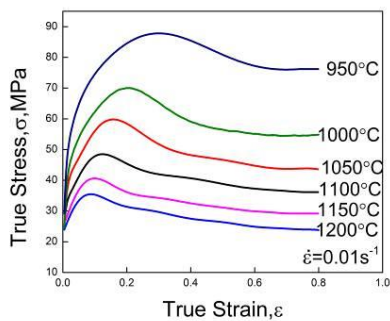


Figure 5.  $\sigma - \epsilon$  curves at  $\dot{\epsilon} = 0.01s^{-1}$

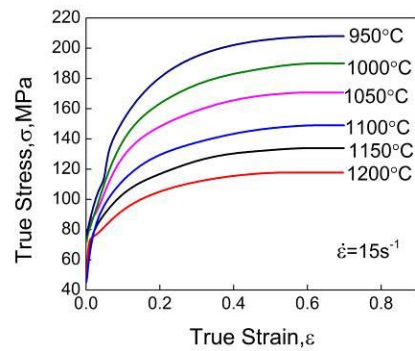


Figure 9.  $\sigma - \epsilon$  curves at  $\dot{\epsilon} = 15s^{-1}$

## 2.2 Model of the flow curves

With regard to the flow curves representing work hardening and dynamic recovery, it is recommended to use the equation (1) to model the flow curves [8].

$$\sigma = B[1 - \exp(-C\varepsilon)]^m \quad (1)$$

where B, C and m are regression coefficients being relevant to chemical composition and deformation parameters. The work hardening exponent m of Equation (1) is normally taken as being a constant. However, as will be seen later, it is a function of the conditions of deformation and of the chemical composition of the austenite. When  $C < 1$ , only work hardening occurs; when  $C > 1$ , both work hardening and dynamic recovery occur [8].

When the flow curves represent hardening, dynamic recovery, and dynamic recrystallization, it is suggested to use the equation (2) to model the flow curves [8].

$$\sigma = B[1 - \exp(-C\varepsilon)]^m - D\{1 - \exp[-k(\varepsilon - \alpha\varepsilon_p/\varepsilon_p)^n]\} \quad (2)$$

where B, C, m, D, k, n and  $\alpha$  are regression coefficients relevant to chemical composition and deformation parameters, and  $\varepsilon_p$  is the peak strain.

## 2.3 Discussion of the $\alpha$ and $\varepsilon_p$

With reference to  $\alpha$ , Medina considered  $\alpha\varepsilon_p$  to be the beginning of the dynamic recrystallization and obtained the values of  $\alpha$  which varied from 0.86 to 0.95 and which remained approximately constant in the published paper [8]. The value of 0.95 was taken as the optimum value for  $\alpha$  due to the fact that with this value the step from the recovery

region to the dynamic recrystallization region was the smoothest [8]. However, Poliak [9] deemed that the  $\alpha$  was between 0.3 and 0.9. In this work, the regression parameter  $\alpha$  was from 0.27 to 1.12. As a result,  $\alpha$  was not taken as a fixed value and the model of  $\alpha$  was built as a function of Z/A. In addition, some values of  $\alpha$  are beyond 1 in this work. It is the problem of software itself. When fitting the data, software was set to obtain the best fitting result without considering the physical meaning of the regression parameters. Furthermore, the best method of calculating the  $\alpha$  value is plotting the  $d\theta/d\sigma - \sigma$  diagram [9, 12]. The  $\alpha$  value of 50A1300 silicon steel was also gained by using this method and consequently the range of  $\alpha$  was consistent with the paper of Poliak [9].

When referring to the  $\varepsilon_p$ , different models were used to model the  $\varepsilon_p$ . For instance, some researchers [12, 13] considered  $\varepsilon_p$  to be the function of the Zener-Hollomon Z, others [7, 9, 14] believed  $\varepsilon_p$  to be the function of the dimensionless parameter Z/A that can be calculated from the hyperbolic equation  $Z = \dot{\varepsilon} \exp(Q/RT) = A[\sinh(\alpha\sigma)]^n$ .

Table 2 shows the values of  $\varepsilon_p$  and Z/A under different deformation conditions. Considering the characteristics of data in Table 2,  $\varepsilon_p = a(Z/A)^b$  was used to model  $\varepsilon_p$  so that the following models were obtained:

$$50A1300: \varepsilon_p = a(Z/A)^b = 0.23350(Z/A)^{0.20620} \quad (3)$$

$$45K-DDQ: \varepsilon_p = a(Z/A)^b = 0.29372(Z/A)^{0.23077} \quad (4)$$

Table 2. The values of  $\varepsilon_p$  and Z/A under different deformation conditions of both steels

Strain rates (s <sup>-1</sup> )		Steel grade	1200°C	1150°C	1100°C	1050°C	1000°C	950°C
0,01	Z/A		0,00768	0,01635	0,03674	0,08781	0,22470	0,62091
	$\varepsilon_p$	50A1300	0,06940	0,08100	0,09840	0,12200	0,14500	0,16407
		45K-DDQ	0,09388	0,10418	0,12187	0,17244	0,20460	0,28407
0,1	Z/A		0,07051	0,14387	0,30919	0,70407	1,71034	4,46748
	$\varepsilon_p$	50A1300	0,13700	0,15900	0,18600	0,21300	0,22100	0,35930
		45K-DDQ	0,16055	0,20160	0,20236	0,24825	0,30803	
1	Z/A		0,41635	0,25000	0,26856	0,41635	0,25000	0,26856
	$\varepsilon_p$	50A1300	0,94328	0,29500	0,31444	0,94328	0,29500	0,31444
		45K-DDQ	2,26823	0,30700		2,26823	0,30700	

**2.4 Modeling the flow curve of 50A1300 silicon steel**

For convenience, before fitting the data, first, we group the flow curves into two categories: the occurrence of dynamic recrystallization (DRX) and no occurrence of DRX. With the use of Origin Pro8.5, regarding to the occurrence of DRX, Equation (2) was applied to fit the data; without occurrence of DRX, Equation (1) was used to fit the data. That is to say that the piecewise fitting method was adopted. The regression parameters B, C, m, D, k, n and  $\alpha$  were obtained in the end. Afterwards, these parameter models as the function of Z/A were built under the principle of accuracy, simpleness and uniformity.

After studying the parameter model in Medina's published paper [8] and by using Quick Fit Function

of 1<sup>st</sup> Opt software package, Equation (5) was obtained, which was the parameter model of 50A1300 silicon steel as the function of Z/A. B, C and m in Equation (1) were substituted by which of Equation (5) in the case of flow curves without DRX. The values B, C, m, D, k, n and  $\alpha$  in Equation (2) were substituted by which of into Equation (5) in the case of flow curves with DRX. Finally, the true stress was gained automatically through writing program under the Matlab environment. A graphic comparison between the measured values and predicted values was shown in Fig. 10(a). A good approximation can be clearly seen, the square of correlation coefficient (R-Square) being 0,979436, and the mean relative error 7,3517%.

$$\left. \begin{aligned}
 B &= (9.87453 + 0.68299 \times \ln(Z/A))^2 \\
 D &= (28.44669 + 427.83896 \times (Z/A)^2 - 956.47522 \times (Z/A)^4) / (1 + 28.25423 \times (Z/A)^2 - 60.42020 \times (Z/A)^4) \\
 C &= (6.03089 - 744.76683 \times (Z/A)^2 + 1635.93360 \times (Z/A)^4) / (1 - 108.03593 \times (Z/A)^2 + 254.15067 \times (Z/A)^4) \\
 m &= (0.16451 + 0.37121 \times (Z/A)^{0.5} - 0.36148 \times (Z/A)) / (1 + 0.40288 \times (Z/A)^{0.5} - 0.84687 \times (Z/A)) \\
 n &= (0.86155 + 0.04880 \times (Z/A)^{0.5} - 0.43662 \times (Z/A)) / (1 - 0.77685 \times (Z/A)^{0.5} + 0.05946 \times (Z/A)) \\
 k &= (0.72283 - 0.14325 \times (Z/A)^{0.5} - 0.37718 \times (Z/A)) / (1 - 1.14891 \times (Z/A)^{0.5} + 0.24119 \times (Z/A)) \\
 \alpha &= 0.94550 + 0.139038 \cos(43.73923 \times (Z/A) + 10.56286)
 \end{aligned} \right\} (5)$$

The accuracy of the parameter model has an effect on the precision of the flow curve model. The more accurate the parameter models are, the more precise the flow curve model is. Especially when the parameter value is bigger than other values, such as B, it has a major influence on the precision of the flow curve model. For this reason, the parameter model B was rebuilt. Equation (6) was obtained

with the help of 1stOpt and then the B values in Equation (1) and Equation (2) were substituted. The square of correlation coefficient (R-Square) between the measured values and predicted values of true stress is 0.987605, and the mean relative error is 5.8802%. It is obvious that the fitting result has been improved.

$$B = \frac{0.0018501 \times (Z/A)^8 + 14.817 \times (Z/A)^6 + 1097.8 \times (Z/A)^4 - 294.58 \times (Z/A)^2 - 69.607}{9.0266 \times 10^{-6} \times (Z/A)^8 + 0.098868 \times (Z/A)^6 + 10.473 \times (Z/A)^4 - 2.0842 \times (Z/A)^2 - 1} \quad (6)$$

**2.5 Modeling the flow curve of 45K-DDQ high-strength steel**

The method of fitting the parameters B, C, m, D, k, n and  $\alpha$  is the same as that of 50A1300 silicon steel. Piecewise fitting method was adopted, and a parameter model was built ((as shown in Equation (7). However, in contrast to (the method of) calculating the true stress of 50A1300 silicon steel, only Equation (2) is used to calculate the true stress of 45K-DDQ high-strength steel. Taken together, both the model and the program were simpler. It is worth noting that the peak strain in the equation (2)

is not always considered as the strain when the peak stress is exhibited. From the DRX flow curve, the peak strain can be calculated as the strain when the peak stress is set up; from the DRV flow curve, the peak strain can be calculated as the maximum strain in the flow curve, i.e., 0.9.

The parameters B, C, m, D, k, n and  $\alpha$  in Equation (2) were substituted into Equation (7). The true stress was gained automatically through writing program in the Matlab environment. A graphic comparison between the measured values and predicted values is shown in Fig. 10(b). Importantly, a good approximation can be seen, the square of

correlation coefficient (R-Square) is 0.974347, and the mean relative error is 6.1453%. In addition, the

result has shown that the changed method is valid.

$$\left. \begin{aligned}
 B &= (9.96861 + 0.62603 \times \ln(Z / A))^2 \\
 D &= 5.9558 \times \cos(22.241 \times (Z / A) - 2.2359) + 25.084 \\
 C &= 2.2818 \times \cos(155.28 \times (Z / A) - 367.31) + 4.7513 \\
 m &= 0.28836 - 0.09699 \times \cos(0.89707 \times (Z / A) - 5.6744) \\
 n &= 1.8613 - 0.9847 \times \cos(5.1503 \times (Z / A) + 24.986) \\
 k &= 0.66492 - 0.45953 \cos(10.127(Z / A) + 340.31) \\
 a &= 222.54 \cos(3.2241 - 0.023159(Z / A)) + 222.8
 \end{aligned} \right\} \quad (7)$$

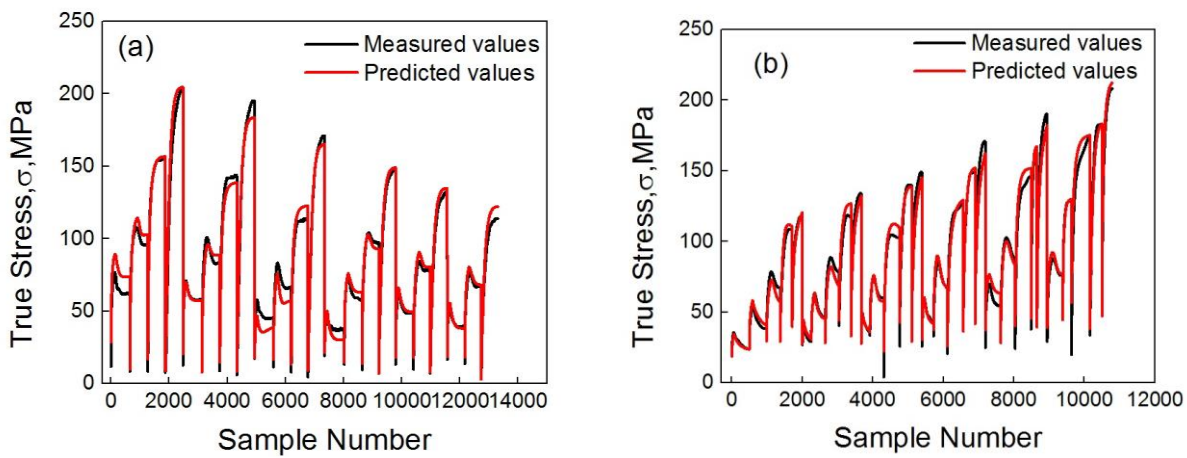


Figure 10. The comparison of predicted stress and measured stress of 50A1300 and 45K-DDQ

## 2.6 Comparison between Piecewise fitting and Global fitting regarding DRX flow curve

As far as the DRX flow curve is considered, two methods could be used, the Piecewise Fitting and the Global fitting. The results mentioned above were gained using the Piecewise fitting method when solving the parameters B, C, m, D, k, n and  $\alpha$ , and the program code is shown as follows.

An attempt was made to compare the Piecewise fitting method and Global fitting method. The parameters of Equation (1) and Equation (2) obtained from Global fitting were different from Piecewise fitting under the same deformation condition. Equation (9) is a program code of Global fitting. Although parameter values calculated by the Global fitting are different from Piecewise fitting,

especially the  $\alpha$  value, the correlation coefficient of the Global fitting is quite high and above 0.98.

Using the Global fitting method and Auto2fit software, the parameters B, C, m, D, k, n and  $\alpha$  were fitted again. Equation (10) is the model and Table 3 is the correlation coefficient of two steels. It is obvious that the correlation coefficient of Global fitting for two steels is bigger than that of a piecewise fitting. And most importantly, only one model was used for B, C, m, D, k, n and  $\alpha$ .

In the 4.3 section, we reached a conclusion that the more accurate the parameter models are, the more accurate the flow curve model is. So, based on the values in Table 3, it is reasonable to conclude that the flow curve model using the Global fitting is more precise than the Piecewise one.

$$\left. \begin{aligned}
 & \text{if } (x < a * p) \\
 & y = B * (1 - \exp(-C * x))^m; \\
 & \text{else} \\
 & y = B * (1 - \exp(-C * x))^m - D * (1 - \exp(-k * ((x - p * a) / p)^n));
 \end{aligned} \right\} \tag{8}$$

Where p is the peak strain  $\epsilon_p$ , x the true strain  $\epsilon$ , y the true stress  $\sigma$ .

$$y = B * (1 - \exp(-c * x))^m - D * (1 - \exp(-k * ((x - p * a) / p)^n)) \tag{9}$$

$$y = p1 + p2 * \cos(p3 * x + p4) \tag{10}$$

where p1, p2, p3 and p4 are fitting coefficient, x the dimensionless parameter Z/A, y the parameter B, C, m, D, k, n and  $\alpha$ .

Table 3. The values of R<sup>2</sup> through the Piecewise fitting and Global fitting method

	R <sup>2</sup>	B	D	C	m	n	k	a	p
Global fitting	45K-DDQ	0,99409	0,99912	0,99905	0,99982	0,99851	0,99923	0,99932	0,99915
	50A1300	0,98064	0,9742	0,99733	0,95179	0,92956	0,94	0,993	0,966
Piecewise fitting	45K-DDQ	0,97551	0,51354	0,62125	0,76458	0,93838	0,83105	0,77673	0,94077
	50A1300	0,97276	0,69614	0,52873	0,84982	0,80396	0,88265	0,78345	0,92263

### 3 Conclusion

The flow models of two steels were built up based on using appropriate changes and modifications. As a result, good approximation results were obtained. Therefore, it is very important to select the appropriate model dependent on certain flow curves. No doubt, the more accurate the parameter models are, the more precise the flow curve model is. The flow curves of 50A1300 silicon steel were modeled using a classification method of the Medina model. The achieved R<sup>2</sup> is 0.979436 and the average relative error is 7,3517%. The flow curves of 45K-DDQ high-strength steel were then modeled using a recrystallization model of the Medina model and the acquired R<sup>2</sup> is 0,974373 whereas the average relative error is 6,1453%. Finally, it is advisable to adopt the Global fitting when fitting the model parameters such as B, C, m, D, k, n and  $\alpha$ .

### Acknowledgements

One of the authors (Lidong, Wang) expresses his thanks to Professor Xudong, Zhou and E. Poliak for their comments and suggestions.

### References

- [1] Zhou, J. H., Guan, K. Z.: *Metal Plastic Deformation Resistance*, China Machine Press, Beijing, 1989, 29-190.
- [2] Liu, J. T.: *The research on hot deformation of model steel*, Shanghai Jiaotong University doctoral dissertation, Shanghai, 1998, 10-32.
- [3] McQueen, H. J., Ryan, N. D.: *Constitutive analysis in hot working*, Materials Science and Engineering A, 322 (2002), 43–63.
- [4] Davenport, S. B., Silk, N. J., Sparks, C. M., Sellars, C. M.: *Development of constitutive equation for modeling of hot rolling*, Mater. Sci. Technol, 16 (2000), 539–546.
- [5] Jorge Jr. A.M., Regone, W., Balancin, O.: *Effect of competing hardening and softening mechanisms on the flow stress curve modeling of ultra-low carbon steel at high temperatures*, Journal of Materials Processing Technology, 142 (2003), 415–421.
- [6] Ebrahimi, R., Zahiri, S. H., Najafizadeh, A.: *Mathematical modelling of the stress–strain curves of Ti-IF steel at high temperature*,

- Journal of Materials Processing Technology, 171 (2006), 301–305.
- [7] Medina, S. F., Hernandez, C. A.: *General expression of the zener-hollomon parameter as a function of the chemical composition of low alloy and microalloyed steels*, Acta Mater, 44 (1996) 1, 137-148
- [8] Hernandez, C. A., Medina, S. F.: *Modelling austenite flow curves in low alloy and microalloyed steels*, Acta Mater, 44 (1996) 1, 55-163.
- [9] Poliak, E. I., Jonas J. J., *Initiation of dynamic recrystallization in constant strain rate hot deformation*, ISIJ International, 43 (2003) 5, 684-691.
- [10] Wang, L. D., Zhou X. D.: *Discussion on the peak stress model of deep drawing high strength steel 45k-DDQ*, Forging and Stamping technology, 37(2012), 5, 150-154.
- [11] Wang, L. D., Zhou X. D.: *Research on flow stress and critical dynamic recrystallization of silicon steel 50A1300*. Journal of iron and steel research, 24(2012), 11, 53-58.
- [12] Jinrong, C., Zhengdong, L.: *Influences of strain rate and deformation temperature on flow stress and critical dynamic recrystallization of heat resistant steel T122*, Acta Metallurgica Sinica , 43 ( 2007), 1, 35-40.
- [13] Najafizadeh, A. Jonas, J. J.: *Prediction the critical stress for initiation of dynamic recrystallization [J]*. ISIJ International, 46 (2006) 11, 1679-1684.
- [14] Zahiri, S. D., Davies C. H. G., Hodgson, P. D.: *A mechanical approach to quantify dynamic recrystallization in polycrystalline metals*, Scripta Materialia, 52 (2005), 299-304.